# Fracture Toughness of Re-entrant Foam Materials with a Negative Poisson's Ratio: Experiment and Analysis

J. B. Choi
and
R. S. Lakes
*Int. J. Fracture*, 80, 73-83, (1996).

ABSTRACT

Fracture toughness of re-entrant foam materials with a negative Poisson's ratio is explored experimentally as a function of permanent volumetric compression ratio, a processing variable. $J_{IC}$ values of toughness of negative Poisson's ratio open cell copper foams are enhanced by 80%, 130%, and 160% for permanent volumetric compression ratio values of 2.0, 2.5, and 3.0, respectively, compared to the $J_{IC}$ value of the conventional foam (with a positive Poisson's ratio). Analytical study based on idealized polyhedral cell structures approximating the shape of the conventional and re-entrant cells disclose for re-entrant foam, toughness increasing as Poisson's ratio becomes more negative. The increase in toughness is accompanied by an increase in compliance, a combination not seen in conventional foam, and which may be useful in applications such as sponges.

## 1. Introduction

Stiff foam is currently used in many load-bearing applications with the aim of optimizing the strength to weight ratio of structural elements. Compliant foam is used in other applications such as seat cushions and sponges. It is therefore important to assess the strength and toughness of the material and to understand the physical causes which govern these properties. Recent studies [1-5] have led to a better understanding of these issues.

Isotropic foam materials with negative Poisson's ratio have been fabricated by one of the authors [6]. Stretching causes an increase in cross-sectional area and compression causes a decrease in cross-sectional area. This behavior is opposite to that of conventional foams which have a positive Poisson's ratio. The interrelation among properties such as flexural rigidity, shear modulus and indentation resistance depends upon Poisson's ratio, consequently negative Poisson's ratio values can give rise to unusual combinations of properties [7-9].

Negative Poisson's ratio materials may also offer advantages in terms of damage resistance, in view of modification of stress concentration factors for inhomogeneities. Stress concentration occurs at discontinuities in a part or member, and alters the stress distribution in that member. The stress at the discontinuity is equal to the product of the nominal stress in the member and the stress concentration factor. Therefore, a lower value of stress concentration factor is highly desirable. The stress concentration factors for a spherical cavity in tension in a plate with infinite thickness are reduced when $\nu<0$; they are increased for a rigid cylindrical inclusion [10, 11]. For a penny shaped crack of radius r in an elastic material [12], the critical stress $\sigma$, which is the stress above which unstable crack growth will occur, goes as $\sigma= \sqrt{[\pi ET/2r(1-\nu^2)]}$ with E as Young's modulus and T as the surface energy. Therefore a sufficiently small negative Poisson's ratio (less than -0.3) is expected to enhance the strength in the presence of cracks, in comparison with 'normal' materials with $\nu \approx 0.3$.

Negative Poisson's ratio materials offer a new direction for achieving unusual and improved mechanical performance. In this study, fracture toughness of conventional and re-entrant copper foams with negative Poisson's ratio is examined experimentally via a standard $J_{IC}$ test which takes the effect of plasticity into consideration. Experimental results are then compared to prior results for foam of conventional structure. Moreover, analytical expressions for the fracture toughness of conventional and re-entrant foams are derived considering the bending moment applied to cell ribs as the foam deforms. This is done based on idealized polyhedral cell structures

approximating the shape of the conventional and re-entrant cells. Tension in the cell ribs will not be important in comparison to bending except in foams with high relative density. Since the cells in foams have a non-zero size, cracks in these materials cannot be perfectly sharp. In this study the crack tip radius is explicitly taken into account.

## 2. Background

The fracture toughness of brittle foam is less well documented than stiffness or strength [13], yet it, too, is important when foams are used in load-bearing applications. Experimentally, Fowlkes [4] and McIntyre [14] have measured the fracture toughness of rigid polyurethane foam and Green [15, 16] examined a lightweight ceramic foam. Maiti et al. [17] used a polyhedral cell model to develop the following analytical expression for the fracture toughness of brittle foam, considering only the bending of the cell rib at a crack tip.

$$\frac{K_{IC}^{*}}{\sigma_f\sqrt{\pi l}} = 0.65\left(\frac{\rho^*}{\rho_s}\right)^{1.5} \qquad (1)$$

where $K_{IC}^{*}$ is the foam fracture toughness, $\rho^*$ is its density, $\rho_s$ is the density of the solid from which the foam is made, $\sigma_f$ is the fracture strength of the cell rib and $l$ is its length. The above authors considered that a crack advanced via the bending failure of the cell ribs; the effect of tension was considered to be second order. The proportionality constant and exponent 1.5 were determined based on the comparison with experimental data. Green [18] derived a similar result (but with a different exponent) by treating the elastic deformation in terms of simple shell theory using a hollow sphere model for the foam cells.

$$\frac{K_{IC}^{*}}{\sigma_f\sqrt{\pi l}} = 0.28\left(\frac{\rho^*}{\rho_s}\right)^{1.3} \qquad (2)$$

However, the rib strength can be dependent on rib volume and the nature of the microstructure within the rib. According to Weibull statistics, a decrease in strength is predicted with increasing volume of material tested, as shown in the work of Brezny et al. [19]. Huang and Gibson applied Weibull analysis to brittle honeycombs [20] and foams [21], leading to a cell size effect for the fracture toughness. By contrast, the above studies by Maiti et al. [17] and Green [18] did not consider this effect and treated $\sigma_f$ as constant at any cell size. Recently, Brezny and Green reported cell size effects in which the strength of vitreous carbon foam was experimentally found to scale inversely with cell size [22]. They attributed this phenomenon to a change in rib strength with size, possibly due to a critical flaw size effect in the ribs.

## 3. Materials and Experimental Methods

The specimens were cut from a large block of open-cell copper foam (Astromet, Inc.) with a high speed saw. Porosity was observed to be fully communicating. The initial relative density ($\rho^*/\rho_s$) of the block was 0.08 ± 5%. Negative Poisson's ratio specimens were prepared by applying sequential plastic deformations in each of three orthogonal directions until the volume was reduced by a factor of from two to four [6]. The ratio of initial volume to final volume is called the volumetric compression ratio and is a processing variable. The size of the specimen should be decided according to the minimum specimen size requirements to ensure nominal plane strain behavior based on linear elastic fracture mechanics. However $K_{IC}$ values for materials similar to the copper foam were not available in the literature. Thus, it was necessary to perform preliminary plane strain fracture toughness ($K_{IC}$) testing to estimate the proper specimen size to obtain a valid $K_{IC}$ value. Compact tension specimens of thickness 19 mm with volumetric compression ratio of

1.0 and 2.0 were made. Tests were performed using a servohydraulic testing machine at a constant displacement rate of 0.3 mm/sec.

Desired fracture specimen thickness, calculated using values of yield strength of the conventional copper foam obtained by a servohydraulic testing (MTS) machine test [23], should be greater than 150 mm. Since the $K_C$ value is dependent upon the specimen thickness, the proper thickness will be between 19 mm and 150 mm. Such a thick specimen is too large to make from available copper foam. In contrast, the required specimen size for a valid $J_{IC}$ test procedure is at least 20 times less than that for a valid $K_{IC}$ test. Moreover, copper is ductile. $K_{IC}$ testing based on linear elastic fracture mechanics ignores plastic deformation. Therefore the $J_{IC}$ test method based on elastic plastic fracture mechanics was chosen.

A thick specimen usually will exhibit a crack tunneling effect in which the portion of the crack beneath the surface advances more rapidly than does the visible crack. As a result it can be difficult to measure the physical crack length. The single specimen technique (elastic compliance method) was therefore used instead of the multiple specimen technique, in which the physical crack length is inferred [24].

For the $J_{IC}$ test, re-entrant copper foams with volumetric compression ratio of 1.0, 2.0, 2.5 and 3.0 were made into compact tension (CT) specimens of thickness 20 mm ± 0.05 mm and width 40 mm ± 0.05 mm. Initial relative density was 0.08 ± 5%. A polymethylmethacrylate (Plexiglas®) piece of thickness 2 mm was bonded at each lateral side to distribute the stress from the applied load and prevent plastic deformation around the pin hole used for specimen fixation. In order to obtain sufficiently sharp crack tips, the specimen was precracked by fatigue. The fatigue process was done at 1 Hz at a force amplitude equal to 25% of the load for plastic collapse as determined from a previous tension test. Total initial crack length was 0.6 of the width. Total crack length in the conventional copper foam was 0.57 of the specimen width. A load cell of 2.5 kN capacity was used to measure force. A load rate of 0.1 N/sec was applied and a clip gage with 8.0 mm working range was used to measure the load-line displacement. Load versus load-line displacement was recorded automatically with an x-y recorder.

## 4. Fracture Toughness of Conventional Foams: Analysis

The load is transmitted through the foam as a set of discrete forces and moments acting on the cell ribs. In brittle foams, since the foam is assumed linear-elastic until the cell ribs fracture, the average force and moment on a given cell rib can be calculated from the stress field in the equivalent classical linear-elastic continuum. All analyses of toughness of foam have used the concept of an equivalent continuum. The discrete problem is solved by taking the solution of the equivalent continuum problem and using it to calculate the force and moments on the discrete cell ribs. The rationale for considering a non-zero crack tip radius in an equivalent continuum representation of foams is shown in Fig. 1, as is a representative cell shape in conventional foams.

A crack of length 2a with crack tip radius $r_{tip}$ in an elastic solid creates the following nonsingular stress field at distance r for $r > r_{tip}/2$ [25] in the continuum view

$$\sigma = \frac{K_I}{\sqrt{2\pi r}} + \frac{K_I}{\sqrt{2\pi r}} \left( \frac{r_{tip}}{2r} \right) \qquad (3)$$

where $K_I$ is the stress intensity factor. Consider the first unbroken cell rib. It is subjected to the following force, in the structural view. The integral is over the thickness of a *rib*, which must bear the load.

$$F = \int_{\frac{r_{tip}}{2}}^{\frac{r_{tip}}{2}+t} \left[ \frac{K_I}{\sqrt{2\pi r}} + \frac{K_I}{\sqrt{2\pi r}} \left( \frac{r_{tip}}{2r} \right) \right] r_{tip}\, dr \qquad (4)$$

A regular tetrakaidecahedron (14 sided polyhedron) is assumed as the mechanical model of the conventional foam cell for analysis since it is the most representative polyhedral cell shape for actual foam materials [13]. For a regular tetrakaidecahedron , the crack tip radius $r_{tip}$ is $\sqrt{2}l$, with $l$ as the rib length.

A Taylor series expansion and a first order approximation is used since the ratio of rib width t to rib length $l$, $t/l$ is very small in low density foams. The force can be expressed as :

$$F = 2.38\, K_I^* \frac{l\sqrt{l}}{\sqrt{\pi}} \left( \frac{t}{l} \right) \qquad (5)$$

where $K_I^*$ is the stress intensity factor of conventional foams.

This force exerts a bending moment on the ribs and the ribs will fail when the stress due to bending moment equals the fracture strength of the cell rib. The maximum theoretical stress, assuming ribs of uniform thickness, occurs around nodes at which cell ribs meet. One would expect the fracture to initiate near the nodes. In reality the ribs of most foams have some taper, and material is concentrated at the nodes, so rib failure can occur elsewhere along the length of the rib.

The stress $\sigma_B$ due to the bending moment is :

$$\sigma_B = 2.12 \frac{F\, l}{t^3} \qquad (6)$$

Using equation (5), $\sigma_B$ becomes

$$\sigma_B = 5.05\, K_I^* \frac{1}{\sqrt{\pi l}} \left( \frac{l}{t} \right)^2 \qquad (7)$$

The crack will extend when $\sigma_B = \sigma_f$, where $\sigma_f$ is the fracture strength of the cell rib. Thus, from equation (7), the fracture toughness $K_{IC}^*$ of conventional foams becomes

$$K_{IC}^* = 0.20\, \sigma_f \sqrt{\pi l} \left( \frac{t}{l} \right)^2 \qquad (8)$$

Since $\rho^*/\rho_S = 1.06\, (t/l)^2$ for a regular tetrakaidecahedron cell,

$$\frac{K_{IC}^{*}}{\sigma_f \sqrt{\pi l}} = 0.19 \left(\frac{\rho^*}{\rho_s}\right) \qquad (9)$$

By contrast Maiti et al. [17] obtained $K_{IC}^* \propto (\rho^*/\rho_s)^{1.5}$ by integrating a singular stress field beginning at zero. The present result was obtained by integrating from a lower limit of $r_{tip}/2 = \sqrt{2}\,l/2$. The rationale is that the actual stress field is not singular in view of the non-zero size of the foam cells. We consider a non-singular field to be physically more reasonable in materials with micro-structure. Comparison with experiment and with other models is given in section 7.

5. Fracture Toughness of Re-entrant Foams: Analysis

Following the same procedure as was used for conventional foams, the fracture toughness of re-entrant foams is obtained. The re-entrant structure is modeled as a re-entrant polyhedron in which the square faces of a regular tetrakaidecahedron protrude inward at the center position of the cell ribs connecting the square faces (Fig. 2). This model was used in obtaining Poisson's ratio of re-entrant foams [26]. For the idealized polyhedron re-entrant cell (Fig. 2), the crack tip radius $r_{tip}$ is approximated by

$$r_{tip} = \left[1 + \sin\left(\frac{\pi}{2} - \phi\right)\right] l, \qquad \frac{\pi}{4} < \phi < \frac{\pi}{2} \qquad (10)$$

The angle $\phi$ determines the extent of the permanent volumetric compression ratio achieved in re-entrant transformation of negative Poisson's ratio foams. The upper limit of $\frac{\pi}{2}$ is an idealization since the ribs have some thickness and do not generate a sharp kink during bending. Moreover, the collapse geometry assumed for the analysis is much more regular than the actual geometry of the foam. With these limitations in mind, the relation between $\phi$, the initial volume $V_i$ and the final volume $V_f$, is

$$\frac{V_i}{V_f} = \frac{48}{5}\sqrt{2}\left[\sqrt{2} + \sin(\pi/2 - \phi)\right]^{-3}. \qquad (11)$$

Solving equation (4), the rib force is expressed as

$$F = 3.37\, K_I^{\,r} \frac{l\sqrt{l}}{\sqrt{1 + \sin\left(\frac{\pi}{2} - \phi\right)}\sqrt{\pi}} \left(\frac{t}{l}\right) \qquad (12)$$

where $K_I^{\,r}$ is the stress intensity factor of re-entrant foams. The stress $\sigma_B$ due to bending for the re-entrant model becomes by equation (12)

$$\sigma_B = 10.10\, K_I^{\,r} \frac{1 + \cos 2\phi}{\sqrt{1 + \sin\left(\frac{\pi}{2} - \phi\right)}} \frac{1}{\sqrt{\pi l}} \left(\frac{l}{t}\right)^2 \qquad (13)$$

The crack will extend when $\sigma_B = \sigma_f$. Thus, the fracture toughness $K_{IC}^{\,r}$ of re-entrant structure becomes

$$\frac{K_{IC}{}^{r}}{\sigma_f\sqrt{\pi l}} = 0.10\,\frac{\sqrt{1+\sin\left(\frac{\pi}{2}-\phi\right)}}{1+\cos 2\phi}\left(\frac{\rho^*}{\rho_s}\right) \qquad (14)$$

Using equation (9), the ratio of fracture toughness of re-entrant foams to that of conventional foams is expressed as

$$\frac{K_{IC}{}^{r}}{K_{IC}{}^{*}} = 0.53\,\frac{\sqrt{1+\sin\left(\frac{\pi}{2}-\phi\right)}}{1+\cos 2\phi} \qquad (15)$$

Cell shape is represented by the angle $\phi$. The divergence for $\phi = 90°$ is not considered physically attainable since the cell ribs have some finite thickness; moreover, real foams have cells of irregular shape which is only approximately represented by the idealized cell shape used in the analysis. Observe that the normalization procedure eliminates the dependence on density.

## 6. Experimental Results and Discussion

As for negative Poisson's ratio materials, the experimental results of $K_{IC}$ tests for copper foam with volumetric compression ratio of 1.0 (corresponding to conventional foam) and 2.0 were 120 kPa$\cdot$m$^{1/2}$, 180 kPa$\cdot$m$^{1/2}$, respectively. Re-entrant foam with volumetric compression ratio of 2.0 exhibited a 50% increase in fracture toughness even though it is more compliant than conventional foam. The experimental results for $J_{IC}$ were 0.8 kPa m for conventional foam and 1.4 kPa$\cdot$m, 1.8 kPa$\cdot$m, 2.1 kPa$\cdot$m for re-entrant foams of volumetric compression ratios of 2.0, 2.5, 3.0. These results correspond to toughness increases of 80%, 130%, 160%, respectively. The experimental results for the relative $J_{IC}$ value are shown in Fig. 3. Also shown is a plot of equation (15) which gives the ratio of fracture toughness of re-entrant foams to that of conventional foams according to a simple model. The model is overly optimistic for volumetric compression ratios of 2.5 and greater. A likely reason is that the model is simple and geometrically regular, while the actual re-entrant foam has a complex and irregular microstructure.

Re-entrant transformation reduces Young's modulus and Poisson's ratio but increases toughness. By contrast for conventional foams stiffness, which goes as $(\rho^*/\rho_s)^2$ following Gibson and Ashby [13], and toughness, which goes as $(\rho^*/\rho_s)^n$ with n = 1, 1.3, or 1.5 depending on the model, are strongly coupled: foams of higher density are both stiffer and tougher than those of lower density. In some applications such as sponges, a combination of compliance (low stiffness) and enhanced toughness may be helpful.

## 7. Discussion and Further Comparisons

As for foams of conventional structure, analytical results for toughness vs relative density (equations (1), (2) and (9)) and experimental results obtained by Fowlkes [4], and by McIntyre [14] are shown in Fig. 4. The analytical results differ in the exponent by which the toughness varies with density. A best fit, based on least squares, to the results of [14] gave $K_{IC}^* = 1.15\,(\rho^*/\rho_s)^{1.786}$. The exponent is larger than that of any of the models. Such a fit, based on absolute deviations, allows larger percent deviations between the fit curve and the experimental data at low density. A second curve fitting to $K_{IC}^*/(\rho^*/\rho_s)^{1.5}$ was performed to evaluate the effect of percent deviations. This gave $K_{IC}^* = 0.706\,(\rho^*/\rho_s)^{1.5004}$, in best agreement with the model of Maiti et al. For higher density foams, the higher terms in the Taylor expansion, which had been neglected,

may become large enough to modify the results. A further complication that foam structure can change with density. Polyhedral cell morphology predominates at low densities [14]. Dense foams tend to be closed-cell, though open cell structure can occur for $\rho^*/\rho_s > 0.3$.

The continuum model used in all the analyses is a classical one which considers force per unit area but not moment per unit area. In some materials with micro-structure, these local moments can give rise to substantial deviations from classical elasticity and can alter the fracture behavior [27]. Most analyses incorporate local moments in the structural view but not in the continuum view, which is contradictory. Cosserat elasticity, which incorporates both a distributed moment as well as a distributed force, has been used in some analyses of fracture. Finally, although experiment suggests an exponent of 1.5, rather than 1.0, a definitive discrimination among the models requires further experiments, since the available experimental results contain considerable scatter and only cover a range of about a factor of ten in relative density. A further analysis incorporating moments in both the continuum and structural views would remove concerns about competing errors.

Analysis of negative Poisson's ratio foams predicts fracture toughness to increase as Poisson's ratio approaches -1. The minimum Poisson's ratio thus far observed is -0.8 at a strain of 0.1% in re-entrant copper foam. Poisson's ratio $\nu_{el}$ at small strain is expressed analytically in terms of rib angle $\phi$ as follows [25]:

$$\nu_{el} = - \frac{\sin(\phi-\pi/4)}{\cos(\phi-\pi/4)} \tag{16}$$

In real materials, cell ribs come into contact at high compression ratio, a fact which is not incorporated in the model. Consequently, the model for fracture toughness does not properly account for the experimental results at or above a volumetric compression ratio of 3. Even above a ratio of 2.5 the model is optimistic in comparison with experiment, since foam cell irregularity is not taken into account. As for the power law in the density dependence, Eq. 15 circumvents uncertainty in the density dependence since normalization procedure eliminates such dependence and leaves only the dependence on rib angle $\phi$.

Re-entrant foam with small volumetric compression ratio is predicted to be less tough than conventional foam. This phenomenon results from the fact that re-entrant foams at low volumetric compression ratio have a smaller absolute Poisson's ratio than conventional foams [26]. Based on Eq. (15), the fracture toughness of re-entrant foams becomes larger than that of conventional foams at a volumetric compression ratio of 1.64 at the same initial relative density.

Another interesting aspect of foam toughness is the relationship between the toughness of the foam and that of the solid from which it is made. In the simplest view, the voids act as built-in crack stoppers. To consider the effect of cell size, suppose the exponent in the toughness equation has a general value n+1 with $n \geq 0$:

$$\frac{K_{IC}^*}{\sigma_f \sqrt{\pi l}} = \left( \frac{\rho^*}{\rho_s} \right)^{1+n} \tag{17}$$

Then, if we suppose $K_{IC} = \sigma_f \sqrt{\pi a}$ is the fracture toughness of bulk material with a through-thickness crack in an infinite plate and 'a' represents a small material defect in the bulk material, the following is obtained.

$$\frac{K_{IC}^*}{\rho^*} = \frac{K_{IC}}{\rho_s} \sqrt{\frac{l}{a}} \left( \frac{\rho^*}{\rho_s} \right)^n \tag{18}$$

Foam toughness can be made much larger than the solid material toughness by increasing the foam cell size. The density term may be equal to or less than one, depending on the model. If a model with $n > 0$ applies, the foam cell size would have to be increased further to achieve a given level of foam toughness. The defect size 'a' also varies among bulk materials, but the cell size $l$ in foams is usually considered to be more under the designer's control. Moreover the defect size 'a' can hardly be as large as the rib thickness t which is less than the cell size $l$. Consequently $l > a$, and with large cell foams we could even have $l >> a$. Results compiled by Ashby [28] include maps of toughness vs density indicate that the fracture toughness of foam materials per unit weight is similar to or even larger than that of bulk materials. Hence foam materials are particularly useful when this kind of property is needed in applications.

Available analytical models differ from the actual structure of cellular solids in several ways. Some foams have a distribution of cell sizes rather than a single repeating unit cell of the same size. Moreover, cells in some foams are slightly flattened or elongated according to the foaming direction, giving rise to anisotropy. These issues should be examined in a further study. Also, it is not clear what to choose for the value of $\sigma_f$, the strength of the cell ribs because the strength is dependent on the volume of the material. It follows, therefore, that modifications need to be made to the theory to interrelate the fracture strength, length, and thickness of ribs. Brezny and co-workers [18] had a preliminary result for the rib strength distribution based on the Weibull modulus. They found that the rib strength was constant with density but showed a substantial increase at the smallest cell size. Huang and Gibson applied the Weibull analysis to honeycombs [20] and foams [21], leading a cell size effect for the fracture toughness. They showed a similar relationship of the cell wall modulus of rupture to the cell size of brittle foam. The copper ribs are ductile even if the foam fails in a brittle way. Ribs which are ductile are likely to yield, bend, straighten, then fail in tension, rather in bending as the model suggest. The model may be more accurate for truly brittle ribs such as ceramics.

The experiments and analysis of negative Poisson's ratio foams apply to the type of foam developed by one of the authors and described in [6]. Other negative Poisson's ratio materials have since been reported [see, e.g. 29-31]; more are given in a recent review [32]; and these deform by different mechanisms and so require independent study.

## 8. Conclusions

Based on the present experimental and modeling studies, the following conclusions are drawn.

1. Fracture toughness of re-entrant foams with a negative Poisson's ratio is observed to be greater than that of foams of conventional foams, even though the re-entrant foams have a smaller Young's modulus.

2. An analytical model of the re-entrant foams accounts for an increase in toughness with transformation processing.

## References

1. M. F. Ashby, *Metallurgical Transactions* A 14A (1983) 1755-1769

2. J. S. Morgan, J. L. Wood, R. C. Bradt, *Materials Science and Engineering* 47 (1981) 37-42

3. D. J. Green, R. G. Hoagland, *Journal of American Ceramic Society* 68 (1985) 395-398

4. C. W. Fowlkes, *International Journal of Fracture* 10 (1974) 99-108

5. P. H. Thornton, C. L. Magee, *Metallurgical Transactions* A 6A (1975) 1801-1807

6. R. S. Lakes, *Science* 235 (1987) 1038-1040

7. R. S. Lakes, *Science* 238 (1987) 551

8. E. A. Friis, R. S. Lakes, J. B. Park, *Journal of Materials Science* 23 (1988) 4406-4414

9. J. B. Choi, R. S. Lakes, *Journal of Material Science* 27 (1992) 4678-4684

10. S. P. Timoshenko, J. N. Goodier, *Theory of Elasticity*, McGraw-Hill, NY (1982)

11. R. E. Perterson, *Stress Concentration Factors*, John Wiley, NY (1974)

12. I. N. Sneddon, *Fourier Transforms*, McGraw-Hill, NY (1951)

13. L. J. Gibson and M. F. Ashby, *Cellular solids* , Pergamon, Oxford, 1988.

14. A. McIntyre, G. E. Anderton, *Polymer* 20 (1979) 247-253

15. D. J. Green, Fabrication and Mechanical Properties of Lightweight Ceramics Produced by Sintering of Hollow Spheres. Final Report on AFOSR contract No. F49620-83-C0078 (1984)

16. D. J. Green, *Journal of American Ceramic Society* 66 (1983) 288-292

17. K. Maiti, M. F. Ashby, L. J. Gibson, *Scripta Metallurgica* 18 (1984) 213-217

18. D. J. Green, *Journal of American Ceramic Society* 68 (1985) 403-409

19. R. Brezny, D. J. Green, C. Q. Dam, *Journal of American Ceramic Society* 72 (1989) 885-889

20. J. S. Huang, L. J. Gibson, *Acta Metallurgica et Materialia* 39 (1991) 1617-1626

21. J. S. Huang, L. J. Gibson, *Acta Metallurgica et Materialia* 39 (1991) 1627-1636

22. R. Brezny, D. J. Green, *Acta Metallurgica et Materialia* 38 (1990) 2517-2526

23. J. B. Choi, R. S. Lakes, *Journal of Materials Science* 27 (1992) 5375-5381

24. *Annual book of ASTM standard*, Designation: E 813-87 and E 1152-87, American Society for Testing and Materials, Philadelphia, PA (1986)

25. H. l. Ewalds, R. J. H. Wanhill, in *Fracture Mechanics 1986*, Edward Arnold, NY (1986) 33

26. J. B. Choi, R. S. Lakes, *Journal of Composite Materials* 29, (1995) 113-128.

27. R.S. Lakes, S. Nakamura, J. C. Behiri, and W. Bonfield, *Journal of Biomechanics*, 23, (1990) 967-975.

28. M. F. Ashby, *Acta Metall.*, 37, (1989) 1273-1293.

29. B.D. Caddock, and K.E. Evans, *J. Phys. D., Appl. Phys.* 22 (1989), 1877-1882.

30. K. L. Alderson, and K. E. Evans, *Polymer*, 33 (1992) 4435-4438

31. A. Y. Haeri, D. J. Weidner, and J. B. Parise, *Science*, 257 (1992), 650-652.

32. R. S. Lakes, *Advanced Materials* (Weinheim, Germany), 5 (1993) 293-296.

Acknowledgment

Support of this research by the NASA/Boeing ATCAS program under contract #NAS1-18889, and by a University Faculty Scholar Award to RSL is gratefully acknowledged.

Figures

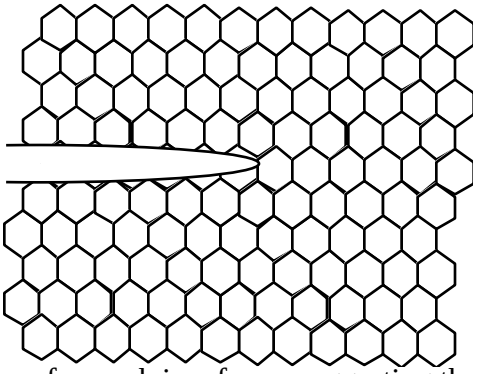

Fig. 1 Structural and continuum views of a crack in a foam, suggesting the use of a non- zero crack tip radius. Detail of crack.

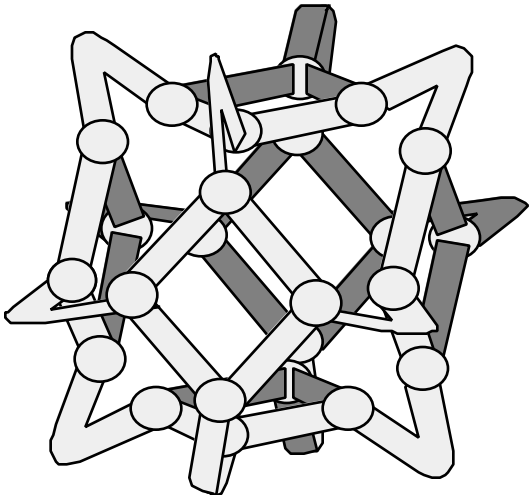

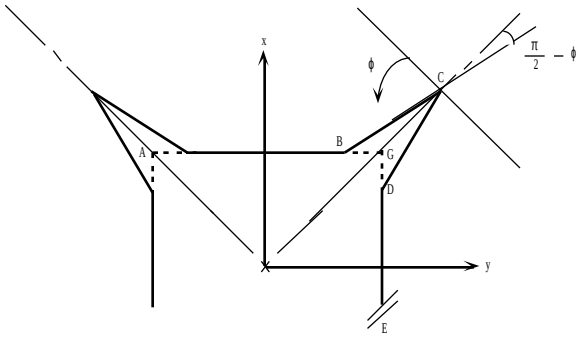


Fig. 2 Top: Collapsed tetrakaidecahedron model for a re-entrant foam cell.
Bottom: Cross section view used for analysis.

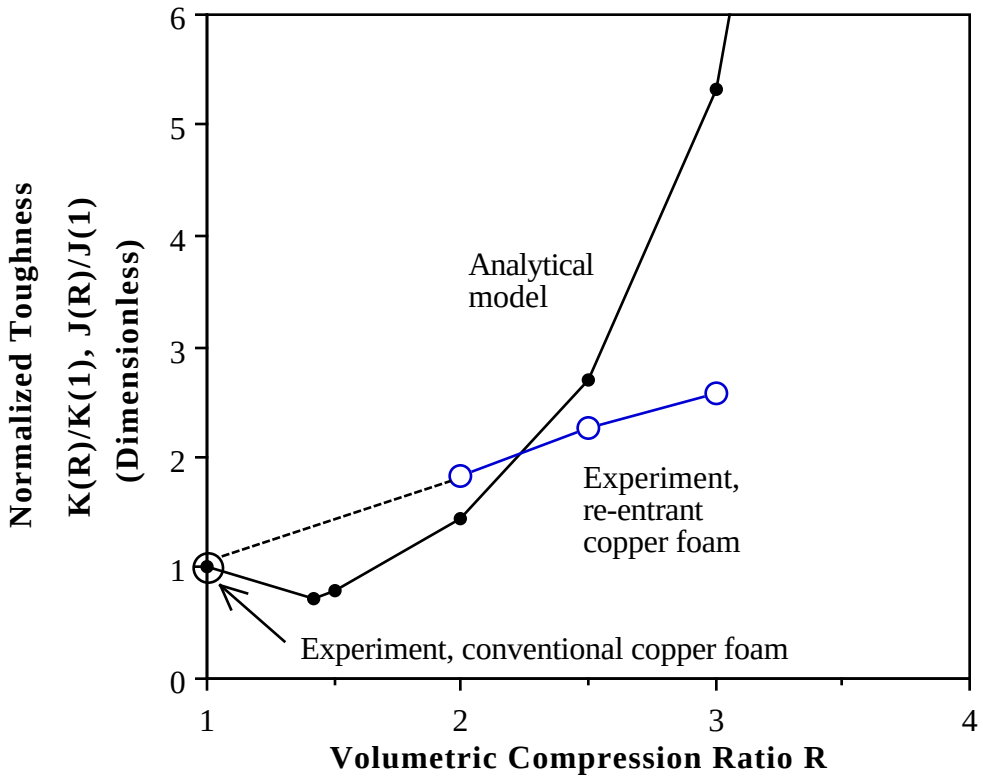


Fig. 3 Experimental $J_{IC}$ results: open symbol, conventional foam; solid symbols, re-entrant foam. The fracture toughness of re-entrant foams is normalized with that of conventional foams, so the ordinate is dimensionless. Analytical result (solid circle, Eq. 15) is shown for comparison.

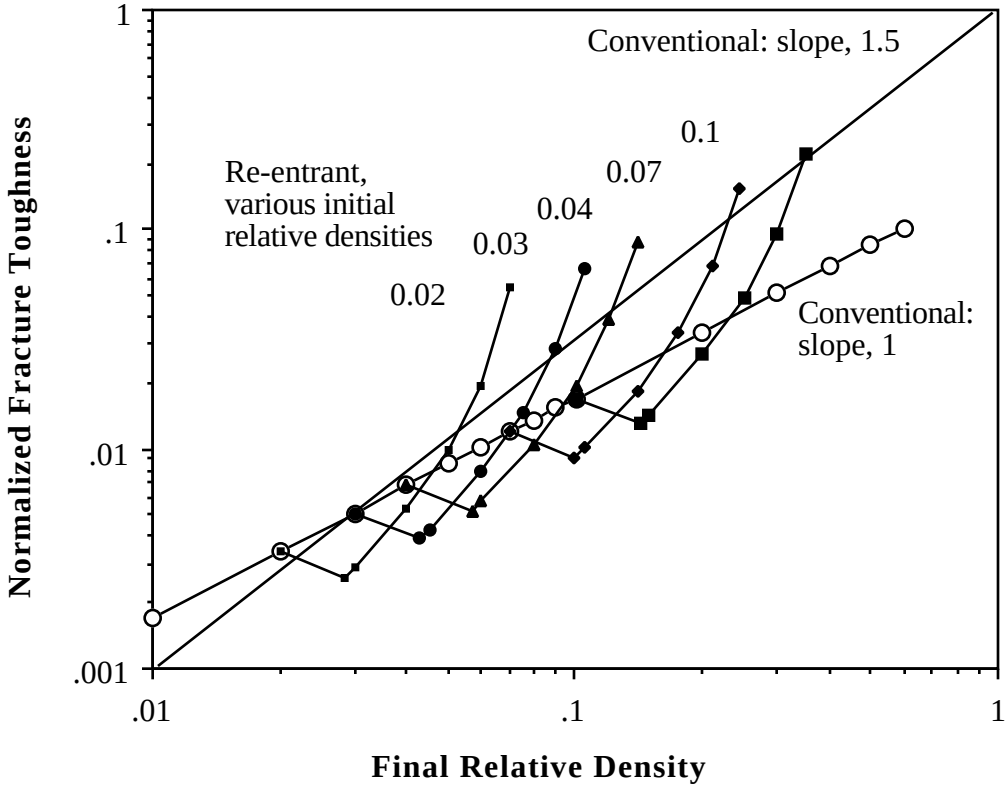
Conventional: slope, 1.5
Re-entrant,
various initial
relative densities
0.1
0.07
0.04
0.03
0.02
Conventional:
slope, 1
Normalized Fracture Toughness
Final Relative Density
1
.1
.01
.001
.01
.1
1

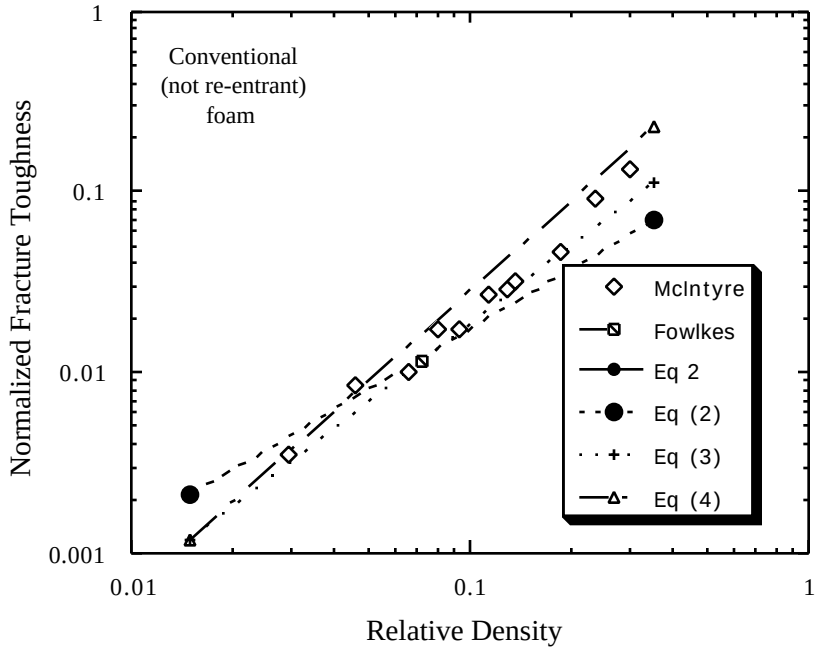
Conventional
(not re-entrant)
foam
McIntyre
Fowlkes
Eq 2
Eq (2)
Eq (3)
Eq (4)
Normalized Fracture Toughness
Relative Density
1
0.1
0.01
0.001
0.01
0.1
1